Electron Spin Resonance Experiments on Donors in Silicon. III. Investigation of Excited States by the Application of Uniaxial Stress and Their Importance in Relaxation Processes

D. K. WILSON*
Bell Telephone Laboratories, Murray Hill, New Jersey

AND

G. FEHER†
University of California, La Jolla, California

(Received June 9, 1961)

The excited states of the antimony, phosphorus, and arsenic impurities in silicon have been investigated by subjecting samples to a uniaxial stress and observing the change in the electron spin resonance spectrum. The experiments were performed at 1.25°K and ~9000 Mc/sec on silicon samples subjected to strains up to 10^{-3}. From the reduction in the hyperfine splitting and the observed g anisotropy under strain the following results were deduced: For a deformation potential of 11 ev, the valley-orbit splitting (i.e., singlet-doublet spacing) for phosphorus was found to be 0.015 ev, for arsenic 0.023 ev, and for antimony 0.013 ev. For the difference in g values with H parallel ($g_{\parallel}$) and H perpendicular ($g_{\perp}$) to the valley axis we obtained for phosphorus-doped silicon, $g_{\parallel}-g_{\perp}=(1.04\pm0.04)\times10^{-3}$.

The observed g shifts with strains along different crystallographic directions revealed the presence of two distinct spin-lattice relaxation (T_s) mechanisms. These were verified and compared with the theory of Roth and Hasegawa. The effect of applied strains on the mutual electron-nuclear spin flip rate (T_x) has been demonstrated. The importance of strain experiments in unravelling relaxation mechanisms is discussed.

I. INTRODUCTION

THE substitutional donors phosphorus, arsenic, and antimony in silicon have one extra unpaired electron which at low temperatures is bound to the donor nucleus. The paramagnetic resonance spectrum of this bound electron has been the subject of several previous investigations[1–4] which helped to elucidate the *ground-state* electronic structure of these so-called "shallow donors."

The present work is concerned with the *excited states* of the localized donor electrons and the effect of admixing these excited states into the ground state by applying a uniaxial stress.

The excited states in question arise in the following way. In the effective mass approximation the donor ground state in silicon is sixfold degenerate—a consequence of the multivalley nature of the conduction band.[5] This degeneracy is lifted by the valley-orbit interaction which splits the six levels into a singlet ground state and a doubly- and triply-degenerate set of excited states. These excited states are important in determining many of the low-temperature properties of silicon. In particular, as we shall see later, they play a dominant role in the interaction of lattice phonons with the donor electron spin system.

Since the optical transitions from the ground state to these excited states is forbidden, it is difficult to obtain their position directly from optical spectra. However, it is possible to determine the position of the excited states by subjecting the silicon lattice to a shear strain which destroys the equivalence of the six conduction-band valleys.[6,7] This has the effect of admixing the doublet state into the singlet ground state. The magnitude of the admixture introduced by the strain was measured in our experiments by observing the corresponding changes in the resonance spectrum.

Experimentally we have observed changes both in the hyperfine splitting and also in the center of gravity of the lines; the latter we term a g shift. From these changes we have determined the splitting of the excited states (i.e., the singlet-doublet separation), the magnitude of the deformation potential for shear, and the nature of the g tensor for an electron in a single valley.

The g shifts due to the applied strain were correlated with the observed spin-lattice relaxation times and compared with the theory of Roth[8] and Hasegawa.[9] Good agreement was obtained between the observed relaxation rate and their theoretical prediction.[10] The presence of an additional relaxation mechanism was revealed by the strain experiments and compared with

* This work was performed in partial fulfillment of the requirements for a Ph.D. degree from Rutgers University, New Brunswick, New Jersey.

† Work performed at the Bell Telephone Laboratories, Murray Hill, New Jersey.

[1] R. C. Fletcher, W. A. Yager, G. L. Pearson, and F. R. Merritt, Phys. Rev. **95**, 844 (1954).

[2] W. Kohn and J. M. Luttinger, Phys. Rev. **97**, 1721 (1955); **98**, 915 (1955).

[3] G. Feher, Phys. Rev. **114**, 1219 (1959); represents Part I of this work.

[4] G. Feher and E. Gere, Phys. Rev. **114**, 1245 (1959); represents Part II of this work.

[5] For a review on this subject, see W. Kohn in *Solid State Physics*, edited by F. Seitz and P. Turnbull (Academic Press, Inc., New York, 1957), Vol. 5.

[6] P. J. Price, Phys. Rev. **104**, 1223 (1956). See in particular footnote 55 of this reference relating to the reduction of the hyperfine interaction by strain.

[7] G. Weinreich and H. G. White, Bull. Am. Phys. Soc. **5**, 60 (1960).

[8] L. Roth, Phys. Rev. **118**, 1534 (1960).

[9] H. Hasegawa, Phys. Rev. **118**, 1523 (1960).

[10] A preliminary account of this work was given by G. Feher, E. Gere, and D. K. Wilson, Bull. Am. Phys. Soc. **5**, 264 (1960).

the theory of Roth.[11] It should be noted that this general approach of correlating strain experiments with relaxation times should be applicable to other paramagnetic systems[12] since in essence one simulates the time-varying effects of a phonon by statically straining the lattice.

II. NATURE OF THE DONOR STATES

A. In the Absence of Strain

The theory of shallow donors has been developed by Kohn and Luttinger.[2,5] They considered the donor electron as moving with an appropriate effective mass m^* in the Coulombic potential of the donor atom imbedded in a dielectric medium. The result of this treatment shows that the Bloch functions, which describe the conduction electrons, are modulated by an envelope function which is the solution of the associated hydrogen-like Schrödinger equation. (The amplitudes for these modulated Bloch functions in a [110] direction are shown in Fig. 6 of reference 3.) Since the appropriate Bloch functions can be taken from any one of the conduction-band minima, the complete wave function must consist of an algebraic sum of Bloch functions from the different minima. Thus they arrive at the following wave function for the donor states:

$$\Psi(\mathbf{r})=\sum_{j=1}^{6}\alpha^{(j)}F^{(j)}(\mathbf{r})u^{(j)}(\mathbf{r})\exp(i\mathbf{k}_0{}^{(j)}\cdot\mathbf{r}), \qquad (1)$$

where $u^{(j)}(\mathbf{r})\exp(i\mathbf{k}_0{}^{(j)}\cdot\mathbf{r})$ is the Bloch function at the jth minimum and $F(\mathbf{r})$ is the effective-mass envelope function. The $\alpha^{(j)}$ are numerical coefficients which describe the relative contribution from each of the different minima or valleys and thereby form different combinations of the wave functions.

Since the effective mass m^* is different for motion of the electrons parallel or perpendicular to the valley, the envelope function is not spherically symmetric. In the case of silicon the wave functions for each of the valleys resemble pancakes with the axis pointing along the direction of the appropriate valley. The Kohn-Luttinger theory of the donor states has essentially been confirmed by both optical absorption and spin resonance studies.[5]

From symmetry considerations the ground state, which would be sixfold degenerate, splits into a symmetric singlet a doublet and a triplet. Only the singlet, which is composed of equal admixtures from each of the valleys, gives rise to a finite probability for the donor electron to be at the donor nucleus. In this region, close to the donor nucleus, the effective-mass approximation breaks down. We therefore expect the doublet and triplet states (whose wave function vanish at the nucleus) to be approximately degenerate and their energy to agree with the effective-mass theory. On the other hand, the simple effective-mass theory will represent a rather poor approximation for the singlet state which has a large probability $|\Psi(0)|^2$ at the donor nucleus. As a consequence of this, the symmetric singlet will be split off from the asymmetric doublet and triplet states. This splitting, which will vary with the donor species is called the "valley-orbit splitting" or the "chemical shift."

Since the hyperfine interaction of the bound donor electron with the donor nucleus depends on $|\Psi(0)|^2$, one expects an appreciable hyperfine interaction for the singlet but none for the doublet and triplet. It is from the observed hyperfine interaction for phosphorus, arsenic, and antimony that one concludes that the ground state in silicon is the singlet for each of these.

B. In the Presence of Strain

If the lattice is now deformed by the application of a uniaxial compressive or tensile stress, the symmetry of the crystal is altered and the equivalence of the valleys is destroyed. Some of the valleys are raised in energy and others are lowered; the magnitude by which they are raised or lowered is of the order $\Xi_u s'=\Xi_u T/C'$, where Ξ_u is the deformation potential for pure shear, T is the stress, and the appropriate elastic constants appear as $C'=\frac{1}{2}(C_{11}-C_{12})$. As a result of the energy difference between the valleys, the ground state will no longer be a pure singlet[6,7] and the relative valley populations will no longer be equal. This "valley repopulating effect" is achieved by admixing some of the excited states. The degree to which these states are admixed depends on the ratio $\Xi_u s'/E_{12}$, where E_{12} is the splitting between the singlet and the doublet. The triplet is not admixed in these static strain experiments because opposite pairs of valleys will move together. The shift in energy of the singlet, doublet and triplet for a stress in a [100] direction is shown in Fig. 1.

The quantitative relation between the energy shifts at different strains is worked out in Appendices A, B, and C. The doublet-triplet degeneracy was lifted in the figure by a small amount E_{23} which, as explained before, is expected to be much smaller than E_{12}.

1. Effect of Strain on the Hyperfine Interaction

As mentioned in the preceding section the wave function of the doublet vanishes at the donor nucleus and consequently does not exhibit a hyperfine interaction. Any admixture of this "hyperfineless" state into the singlet ground state will therefore reduce the observed hyperfine splitting. If one assumes that the only effect of the strain is to alter the valley populations, one can solve the associated Hamiltonian exactly. This has been done in Appendix D for an arbitrary stress in the [100] direction. The result for the ratio of the

[11] L. Roth, Massachusetts Institute of Technology Lincoln Laboratory Reports, April, 1960 (unpublished).

[12] E. S. Rosenvasser and G. Feher, Columbia Radiation Laboratory Report, August, 1960 (unpublished) describe the effect of strain on the electron spin resonance pattern of Fe^{3+} and Mn^{++} in MgO.

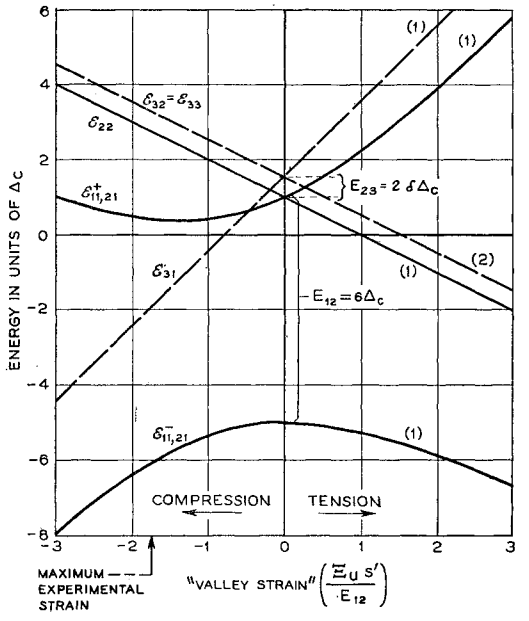

FIG. 1. Energy of the various 1s-like donor levels in silicon (with respect to the energy center of gravity) versus the "valley strain" $\Xi_u s'/E_{12}$ with an uniaxial stress applied in the [100] direction. Energies are expressed in units of $\Delta_c=\frac{1}{6}$ the singlet-doublet splitting E_{12}. The doublet triplet splitting E_{23} is assumed small in comparison to E_{12}. The numbers in parenthesis indicate the degeneracy of the level. The analytical expression of the energy levels versus strain are derived in Appendix C.

hyperfine splitting with strain $(\text{hfs})_s$ to the unstrained value $(\text{hfs})_0$ is given by

$$(\text{hfs})_s/(\text{hfs})_0=\tfrac{1}{2}\{1+(1+x/6)(1+x/3+x^2/4)^{-\frac{1}{2}}\}, \quad (2)$$

where x is called the "valley strain" and is given by

$$x=\Xi_u s'/E_{12}. \quad (3)$$

At very small strains ($x\ll 1$) this result shows the change in hyperfine splitting with strain to be quadratic. This is easily seen from perturbation theory since the doublet state which is admixed by the strain vanishes at the donor nucleus and therefore, one would not expect a first-order change in the ground-state wave functions at the origin.[5] (The hfs with the Si^{29} nuclei would of course exhibit a first order change with strain.) In our experiments the strains are rather large and the observed changes in the hyperfine splitting are appreciable. For extremely large strains one can define two limiting cases[6]: Under uniaxial compression, the strain is negative and since Ξ_u is a positive quantity, expression (2) will reach a limiting value of $\frac{1}{3}$; this corresponds to the donor electrons spending all of their time in the two depressed valleys as compared to the six original ones. Under uniaxial extension, the strain is positive and a limiting value of $\frac{2}{3}$ is reached; i.e., only four of the six valleys are occupied. Although we did no actual experiments of the second type, they were in essence simulated by compressive stresses applied in the [110] direction. This also depresses four of the valleys and raises the other two. Our largest [100] compressions, with strains of the order of 10^{-3}, correspond to the electrons spending 60% of their time in the two depressed valleys.

2. *Effect of Strain on the g Shift*

In addition to the hyperfine splitting, the electron spin-resonance spectrum is also characterized by the position of its center of gravity which is determined by the g value of the electron. The field at resonance is given by

$$h\nu=g\mu_0 H, \quad (4)$$

where μ_0 is the magnetic moment of the electron, H is the magnetic field, ν is the applied microwave frequency, and g is the electronic g factor which in general may depend on the orientation of the magnetic field H.

In order to understand the effect of strain on the observed g value, let us consider the hypothetical case of having all the electrons in one valley. Since the g is a measure of the spin-orbit interaction and the orbit of an electron in a valley is different whether it moves parallel or perpendicular to the valley axis one would expect to observe an anisotropic g value. It can be easily shown[13] that for this case the electronic g value is given by the relation

$$g^2=g_{11}^2\cos^2\theta+g_\perp^2\sin^2\theta, \quad (5)$$

where θ is the angle between the applied field and the valley axis and g_{11} and $g_\perp$ are the g values with the magnetic field pointing parallel and perpendicular to the valley axes.

If one wants to calculate the g value for a real case, i.e., for an electron in a given donor state, one has to take a suitable average of the above expression over the different valleys. For the singlet, one finds that the average g is isotropic and is given by[8] (see Appendix E)

$$g_0=\tfrac{1}{3}(g_{11})+\tfrac{2}{3}(g_\perp). \quad (6)$$

a. g shift due to valley repopulation. Under the application of a uniaxial stress the six valleys will not be equally populated and averaging expression (5) over all the valleys will not result in an isotropic g value. This is just a consequence of the fact that the doublet state which the strain admixes into the ground state is not isotropic. In Appendix F we derive the expression for the g shift due to this valley repopulation effect with the stress applied along the [100] direction.

$$g-g_0=\tfrac{1}{6}(g_{11}-g_\perp)(1-\tfrac{3}{2}\sin^2\theta)\times[1-(1+3x/2)(1+x/3+x^2/4)^{-\frac{1}{2}}], \quad (7)$$

where g is the observed g value under strain, g_0 is the unstrained value, θ is the angle between the stress axis and the magnetic field, and x is the "valley strain" as defined before. Thus by fitting the experimentally ob-

[13] See for instance: W. Low, *Paramagnetic Resonance in Solids* (Academic Press, Inc., New York, 1960), p. 53.

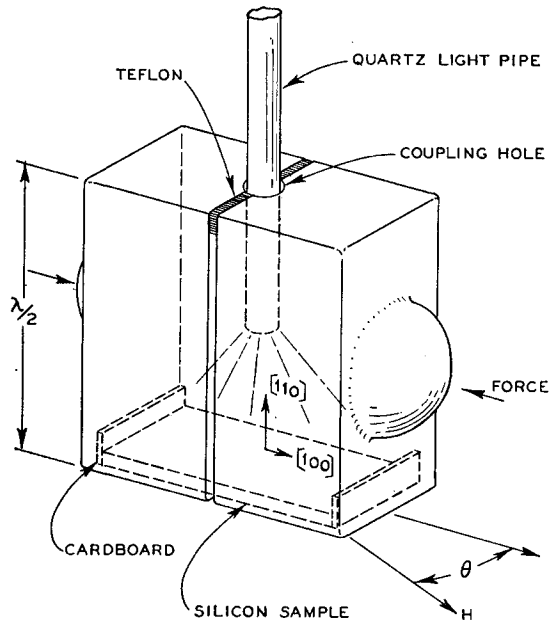

FIG. 2. Microwave cavity assembly with silicon sample. The load is applied to the hemispheres (see Fig. 3) and is shared by the sample and the Teflon strip which surrounds the coupling hole. The silicon samples are slightly longer than the inside dimension of the cavity. The quartz light pipe provides illumination for the sample which reduces the relaxation times.

served g values at different strains with expression (7) one obtains the parameters $g_{\parallel}$ and $g_{\perp}$. (See IV, B).

b. g shift within one valley. The values of $g_{\parallel}$ and $g_{\perp}$ can be calculated from the momentum matrix elements and spin-orbit splittings of the nearby energy bands. The nearest band to the conduction-band minima is the Δ_2' band; however its matrix elements vanish in the absence of strain. In the presence of strain, this band will admix and give rise to a g shift which would be observed even if all the electrons were confined to one valley.

Roth[11] has shown that such a g shift can arise from an interaction H_2 which has the form

$$H_2=\tfrac{1}{2}A\mu_0[\epsilon_{xy}(S_xH_y+S_yH_x)+\text{cycl. perm.}], \quad (8)$$

where ϵ_{xy} is the xy component of the strain tensor and A involves the relevant matrix elements as given by Roth.[11]

The interaction H_2 gives rise to an anisotropic g shift which can be expressed by the relation[14]

$$g-g_0=\tfrac{1}{3}A(T/C_{44})(1-\tfrac{3}{2}\sin^2\theta), \quad (9)$$

where g is the observed g value, g_0 is the unstrained value, T is the stress applied in the [111] direction, C_{44} is the elastic constant (for silicon,[15] $C_{44}=8\times10^{11}$ dynes/cm^2), and θ is the angle between the stress axis and the magnetic field H which is rotated in the (110) plane.

[14] Y. Yafet (private communication).
[15] H. J. McSkimin, J. Appl. Phys. 24, 988 (1953).

In general both g shifts will be observed simultaneously. However, by choosing a particular stress axis, the two effects can be separated out (see Sec. IV, B).

III. EXPERIMENTAL DETAILS

A. Experimental Equipment

The electron spin-resonance spectrometer used in these experiments is a balanced bridge type and employs a superheterodyne detector.[16] The experiments were performed at ~9000 Mc/sec and a temperature of 1.25°K. At these low temperatures and the low donor concentrations used,[17] the spin-lattice relaxation times become prohibitively long. In order to relax the spin system more rapidly, free carriers were introduced by flooding the sample with light[4] guided down the waveguide by means of a quartz rod. All observations were made under adiabatic fast passage conditions[18] with the bridge tuned to the dispersion mode. A 100-cps field modulation was used.

The rectangular microwave cavity operates in the TE_{101} mode mode and is shown in Fig. 2. It consists of two quarter-wave sections molded from Pyrex glass and coated with silver paint. Hemispheres are ground on the outside faces of the split sections. The silicon samples are slightly longer than the inside dimensions of the cavity so that a force applied to the hemispheres is transferred to the sample. Cardboard or Teflon is placed between the sample and the cavity. The cardboard plastically deforms under the applied stresses and distributes the stress uniformly over the cross-section of the sample. The spacing between the halves of the cavity when the sample is loaded is of the order of 0.5 mm. Since the slit is parallel to the microwave current lines, the Q of the cavity is not affected adversely by this spacing.

The mechanical arrangement for transmitting the forces down the Dewar to the cavity is shown in Fig. 3. A large adjustable calibrated spring exerts a maximum tensile force of 25 kg on a flexible copper wire, which is coupled through a vacuum bellows to a pivoted lever arm which applies the force to the cavity. The jaws of the lever have hemispherical holes slightly larger in diameter than the hemispheres on the cavity walls so that when the system is assembled, the cavity centers itself. This assures that the forces on the cavity and hence on the sample are uniaxial. In this arrangement the dc magnet field may be rotated to have its direction parallel to the applied stress. We call this device the "parallel squeezor." A similar arrangement rotated through 90° is used for applying forces perpendicular to the magnetic field (the "perpendicular squeezor"). It is shown on the right side of Fig. 3.

[16] G. Feher, Bell System Tech. J. 26, 449 (1957).
[17] Donor concentrations of ~10^{16}/cm^3 were used. For phosphorus-doped silicon at 1.25°K this results in a spin-lattice relaxation time of about an hour. (See reference 4.)
[18] See Appendix of reference 3.

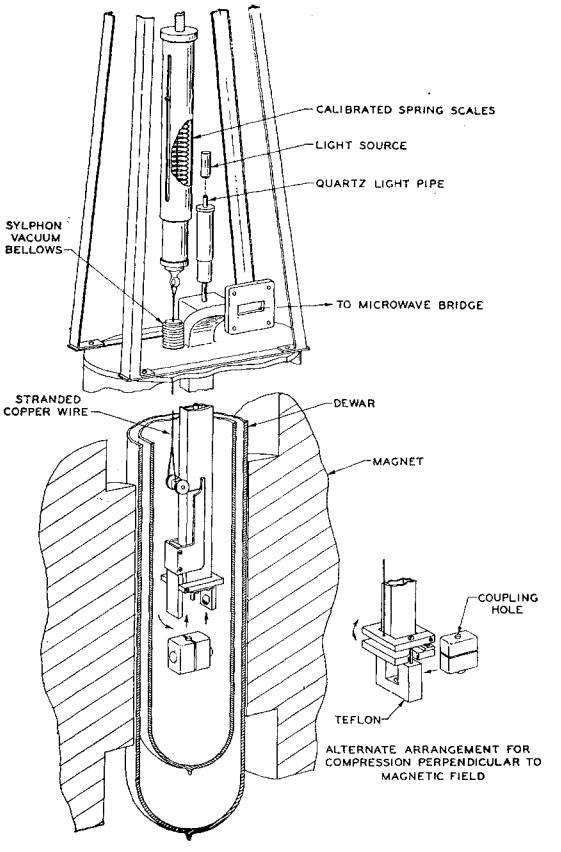

FIG. 3. Mechanical assembly used to apply stress to silicon samples at liquid helium temperatures. The assembly shown within the Dewar is called the "parallel squeezor" since the stress can be applied in the direction of the magnetic field. The alternate arrangement for compression perpendicular to the field is called the "perpendicular squeezor" and is illustrated in the lower right-hand corner.

B. Determination of Strain

The force on the cavity may be obtained by measuring the exact dimensions of the lever arms and calibrating the spring with known weights. A more direct method which we used for our final stress determination was to measure the deformation of calibrated hardened steel rings inserted in place of the cavities. In this way the two lever arms of the squeezing arrangements were found to have mechanical advantages of 4.40 and 2.10, respectively. The load necessary to overcome vacuum loading of the bellows, binding, and other nonlinear effects in the mechanical system introduces an error of $\sim 3\%$ into the calculation of strain in the sample.

Within the microwave cavity the load is equally shared by the sample and the Teflon spacer at the opposite end of the cavity. Since the maximum load applied by the calibrated spring is 25 kg, the maximum load on the sample is 62.5 kg for the "parallel squeezor" and 26 kg for the "perpendicular squeezor." The elastic constants C_{11} and C_{12} for silicon at 1.25°K were extrapolated from the low-temperature measurements of McSkimin.[15] The resultant value for C' is 0.522×10^4 kg/mm^2.

The silicon samples were cut from Czochralski-grown crystals of approximately 10^{16} N_d/cm^3 and oriented with an x-ray goniometer to within 20′ of the appropriate axis. They were cut to dimensions of 0.75 mm$\times$9 mm$\times$22 mm and lightly etched.[19] The etching reduces the surface recombination and thereby increases the effectiveness of the light in relaxing the spins. After etching, the cross-sectional area was accurately measured.

The main error in the determination of the strain arises from strain gradients within the sample due to a nonuniform stress distribution at the ends. We have estimated these strain gradients in the following way: We have shown that uniaxial compression produces a g shift proportional to strain (provided $g_{11}\neq g_1$). If the strain varies across the sample, the resonance condition will vary from region to region resulting in a broadening of the resonance line. The strain gradient can then be estimated from the ratio of the strain-broadening of the line to the strain shift of the same line. Since these quantities are extremely small for silicon, the estimates were made using arsenic-doped germanium for which the g shifts are three orders of magnitude larger.[20,21] For

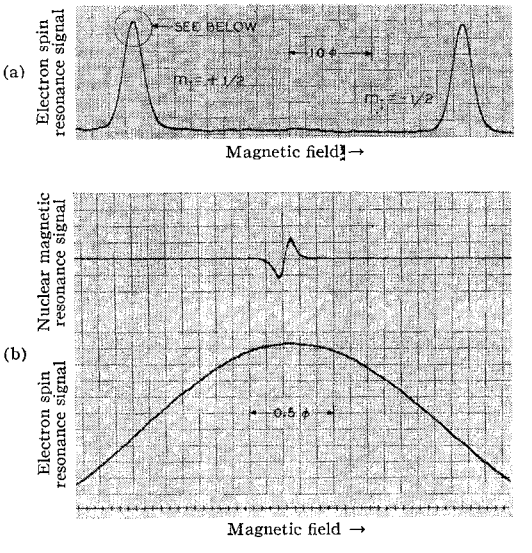

FIG. 4. Illustration of the method used for the accurate determination of the hfs and the electronic g value. (a) Hyperfine spectrum of phosphorus donors in silicon; $N_d=10^{16}$/cm^3, $T=1.25$°K $\nu_e\simeq 9$ kMc/sec. (b) Portion of the $m_I=+\frac{1}{2}$ line which is shown encircled in (a). The field marker shown is derived from a proton sample. The centers of the lines were determined with an accuracy of $\sim$10 millioersteds.

[19] The etch consisted of three parts (by volume) of nitric and one part of hydrofluoric acid. The samples were etched at room temperature for about one minute.

[20] D. K. Wilson and G. Feher, Bull. Am. Phys. Soc. **5**, 60 (1960).

[21] D. K. Wilson and G. Feher (to be published); G. Feher in *Proceedings of the International Conference on Semiconductor Physics, Prague, 1960* (Publishing House of the Czechoslovak Academy of Sciences, Prague, 1961), p. 579.

most of our runs we found strain gradients of the order of 5%. We estimate the over-all error in the determination of the strain to be approximately 6%.

C. Experimental Procedure

The basic quantity which had to be measured was the shift of the center of the electron spin resonance line at different stresses and angles. In order to achieve this, a linear magnetic field sweep extending over only a small portion of the linewidth was used. (see Fig. 4). Superimposed on the linear sweep was the usual 100 cps field modulation with a peak-to-peak value not exceeding 0.1 oe. The centers of the lines were made to coincide with magnetic field markers derived from a nuclear resonance probe. The dc magnetic field and the NMR frequency were kept constant throughout an experimental run so that changes in the spin spectrum were observed as displacements of the peaks from the NMR marker. The accuracy of the measurement was of the order of 10 millioersteds. Since the hyperfine splittings at maximum strains were reduced by several oersteds, the accuracy with which *changes* in the hfs could be measured was less than 1%. The displacement of the lines due to the strain-induced g shifts never exceeded a fraction of an oersted, which reduced the accuracy of the g-shift determination to about 3%.

In measuring the g shifts as a function of angle, a correction for the changing demagnetization of the cavity walls had to be applied. These demagnetization values varied by about 30 millioersteds and were obtained by measuring the apparent g shifts in an unstrained sample.

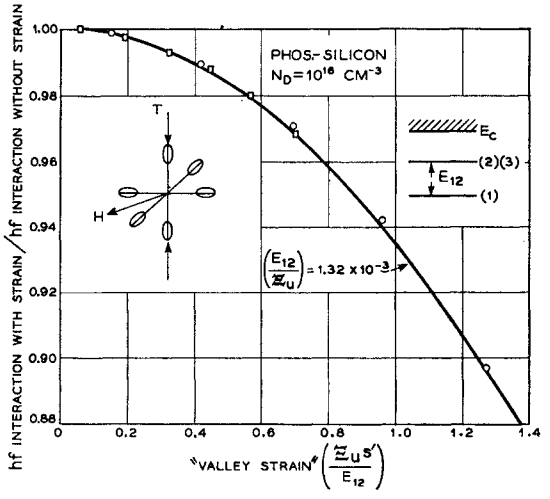

FIG. 5. Ratio of the hyperfine splitting with strain to the unstrained value as a function of "valley strain" $\Xi_u s'/E_{12}$ for uniaxial compression in a [100] direction. The sample is phosphorus-doped silicon at 1.25°K and $\nu_e \simeq 9$ kMc/sec. At the largest valley strains, the donor electrons are spending approximately 60% of the time in the depressed valleys. The solid curve represents the fit with Eq. (2), assuming $E_{12}/\Xi_u = 1.32\times10^{-3}$.

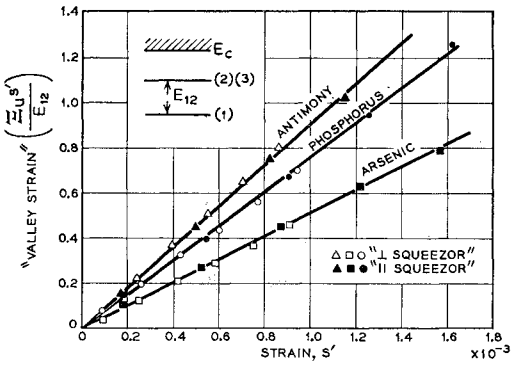

FIG. 6. "Valley strain" $\Xi_u s'/E_{12}$ determined by means of Eq. (2) from the changes in the hfs versus elastic strain $s'=2(s_{11}-s_{12})T$ for a uniaxial compression in the [100] direction. Temperature $=1.25$°K, $\nu_e=9$ kMc/sec, $N_d \approx 10^{16}$/cm^3. The lines are drawn for the values of E_{12}/Ξ_u listed in Table I.

All our measurements were based on the observed displacements of the $m_I=-\frac{1}{2}$ and $m_I=+\frac{1}{2}$ lines, and in the case of antimony-doped samples only those of the Sb^{123} isotope. The hyperfine splitting is then obtained directly to second order from the separation of these two lines. (See discussion of the Breit-Rabi formula in Appendix G.) The g factor is determined from the center of gravity of the two lines, subject again to the Breit-Rabi correction.

IV. EXPERIMENTAL RESULTS

A. Determination of E_{12} from the Reduction in the Hyperfine Splitting

The reduction in the hyperfine splitting at different valley strains $\Xi_u s'/E_{12}$ is shown in Fig. 5. The results were obtained on a phosphorus-doped silicon sample subjected to an uniaxial compression in the [100] direction. The solid curve represents a fit with the theoretical expression [Eq. (2)] assuming for the ratio E_{12}/Ξ_u a value of 1.32×10^{-3}.

An alternate way of presenting the data is to calculate by means of Eq. (2) for each point the appropriate valley strain x. Figure 6 shows the results of this procedure for the three donors; antimony, phosphorus, and arsenic. The experimental results were obtained with both the parallel and perpendicular squeezor (see Sec. III, B). The straight lines indicate the validity of Eq. (2) and provide a strong evidence that the changes in $|\Psi(0)|^2$ are due to the "valley-repopulation effect." The values for E_{12}/Ξ_u obtained from the slopes of the lines are presented in Table I. In order to obtain the singlet-doublet splitting E_{12}, the deformation potential Ξ_u has to be known. Unfortunately there are no suitable experimental values available at present[22]; a theoretical estimate by Herring[23,24] places it in the range

[22] Cyclotron resonance experiments under uniaxial stress are presently being performed in order to obtain an independent value of Ξ_u [J. C. Hensel and G. Feher (to be published)].

[23] C. Herring, Bull System Tech. J. **34**, 237 (1955).

[24] C. Herring and E. Vogt, Phys. Rev. **101**, 944 (1956).

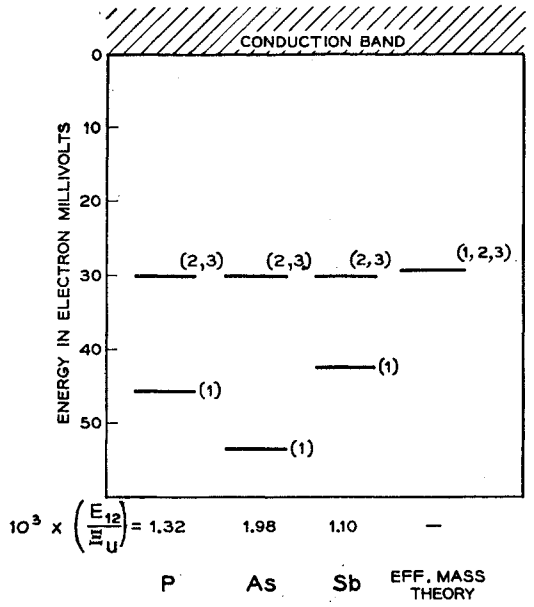

FIG. 7. Energy level scheme for the donor electron with 1*s*-like wave functions in phosphorus-, arsenic-, and antimony-doped silicon. Scheme is based on the assumption that doublet is independent of the donor species. This yields for the deformation potential a value of $\Xi_u=11$ ev. The separation of the doublet and triplet is not determined in our experiments and is assumed to be small compared to the splitting E_{12}.

between 7 and 11 ev. The positive sign of Ξ_u was verified in our experiments by observing a larger change in the hfs under a compressive stress in the [100] direction than under a similar extensive stress (simulated by a compressive stress in the [110] direction).

Lacking a precise value for the deformation potential, we deduced its value from our experimental data in the following way: Since the wave function for the doublet state vanishes the donor nucleus, its energy level should be determined to a good accuracy by the effective-mass theory.[5] The position of the level will then be *independent* of the donor species. There is evidence from optical absorption measurements that this is the case for most of the excited states that similarly vanish at the donor nucleus.[5] On the basis of this assumption one can calculate Ξ_u from the optical ionization energies[5,25]

TABLE I. The singlet-doublet splitting E_{12} for different donors obtained from the hyperfine splitting under uniaxial compression. Note that in order to get E_{12}, the deformation potential Ξ_u has to be known. By assuming the validity of the effective mass theory for the doublet state, a value of $\Xi_u=11$ ev was deduced.

Donor	Ionization energy[a] (ev)	E_{12}/Ξ_u	E_{12}(ev)
Phosphorus	44.6×10^{-3}	$(1.32\pm0.08)\times10^{-3}$	15×10^{-3}
Arsenic	52.5×10^{-3}	$(1.98\pm0.12)\times10^{-3}$	22×10^{-3}
Antimony	43×10^{-3}	$(1.10\pm0.07)\times10^{-3}$	12×10^{-3}

[a] See references 5 and 25.

[25] N. B. Hannay, *Semiconductors* (Reinhold Publishing Corporation, New York, 1959), p. 460.

of the singlet and our experimental values of E_{12}/Ξ_u. The average value of the deformation potential obtained in this way is $\Xi_u=11\pm1$ ev. This places the doublet $(30.0\pm1.0)\times10^{-3}$ ev below the conduction band, in very good agreement with the theoretical effective-mass value[2] of 29×10^{-3} ev. Table I lists the optical ionization energies of the singlet level and the singlet-doublet splittings E_{12}. The relative positions of the singlet and doublet estimated in this way for all three donors is shown in Fig. 7. The value obtained for the splitting in phosphorus-doped silicon (15×10^{-3} ev) is consistent with that obtained from Hall measurements by Long and Myers.[26]

B. Electronic *g* Shifts

As we have discussed in Sec. II, there are two mechanisms that give rise to a *g* shift under strain. One is due to the repopulation of the valleys (caused by the admixture of the doublet), the other is due to the strain dependence of $g_{\parallel}$ and $g_{\perp}$ themselves (caused by the change in the matrix element which admixes higher lying bands). The experimental problem is to measure these shifts independently. This is possible by applying the stress along two different crystallographic directions. Roth has shown[11] that the "one-valley effect" arising from the admixture of the Δ_2' band (see Sec. IIB, 2b) should be absent when the stress is applied along the [100] direction. The "repopulation effect," on the other hand, disappears with stresses applied in the [111] direction. This is evident from the fact that for this stress direction the angles between each of the [100] valley axis and the stress axis are equal. As a consequence all valleys shift by the same amount and no repopulation occurs.

1. g shift due to valley repopulation. In Sec. II B we presented the relation [Eq. (7)] between the *g* shift and the applied strain. This expression [Eq. (7)] suggests two possible experimental procedures to evaluate $g-g_0$. One can either keep the magnetic field at a fixed angle and vary the valley strain or alternately vary the angle θ for a given value of x. In the latter procedure one has to make a correction (see Sec. IV A) due to the varying demagnetization factor but gains a small convenience by not having to evaluate the Breit-Rabi correction at each angle. This correction has to be reevaluated for each strain value since the hyperfine splitting is strain dependent. Having determined this dependence (see previous section), it incidentally provides a convenient strain calibrator.

We have performed both type of experiments. Figure 8 shows the experimental results of $g-g_0$ vs the applied valley strain. They were obtained in the "parallel squeezor" with T along the [100] direction and H pointing always perpendicular to it. The experimental points represent averages of three different runs taken with H along the [010] direction, along the [001]

[26] D. Long and J. Myers, Phys. Rev. **115**, 1119 (1959).

direction, and at 45° to both the [010] and [001] directions. The full line represents a theoretical fit with $g_{\parallel}-g_{\perp}=1.1\times10^{-3}$. Similar results were obtained on antimony- and arsenic-doped silicon. Since at large values of strain only the valleys in the direction of the stress will be occupied, we expect that g under strain will approach $g_{\perp}$. From the observed decrease in g under strain we conclude that $g_{\perp}<g_{\parallel}$.

The g shifts at constant strains versus the angle θ were measured in the "parallel squeezor." The experimental results on arsenic-doped silicon as well as the crystallographic orientation of the sample are shown in Fig. 9. As expected from symmetry, the g shifts vanish in the [111] direction.

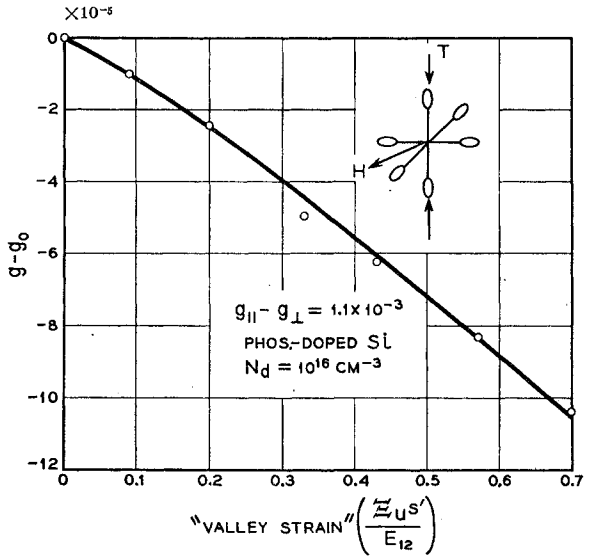

FIG. 8. g shift vs the valley strain in phosphorus-doped silicon; $T=1.25$°K, $\nu_e=9$ kMc/sec. Uniaxial compression applied in the "perpendicular squeezor" along the [100] direction. Points are average shift for magnetic field in the [010], [001], and [011] crystallographic directions, normal to applied stress. The solid curve represents the fit with Eq. (7) assuming a value for $\Delta g=g_{\parallel}-g_{\perp}=1.1\times10^{-3}$.

The values for $g_{\parallel}-g_{\perp}$ obtained from these two sets of experiments agree with each other and are listed in Table II.

Roth[8] has calculated the g values for silicon from the known energy-band parameters using a two-band model. Her calculations indicate $g_{\parallel}-g_{\perp}$ to be approximately -3×10^{-3} and $(g_{\perp}-2)$ to be about $\frac{1}{6}(g_{\parallel}-2)$. This is in contradiction with the experimental values, which, as pointed out by Roth and Liu and Phillips,[27] is due to the limitations of the two-band calculation. More recently, Liu and Phillips[27] have calculated all matrix elements for silicon and their value for $g_{\parallel}$ and $g_{\perp}$ agree with experiment to within $\sim10\%$.

2. g shift within one valley. If we apply a stress in the [111] direction, no repopulation of the valleys takes place and the observed g shift will be due to the one-valley effect. The experimental results are shown in Fig. 10 where $g-g_0$ is plotted versus $\sin^2\theta$ for three different strains.

The g shifts were found to be the same for all three donors. This indicates that the bands which are mixed in by the applied strain are displaced in energy by an amount large in comparison to the singlet doublet splitting E_{12}. This is to be expected from Roth's[11] theory which assumes Δ_2' to be responsible for this g shift.

By comparing the experimental results of Fig. 10 with expression (9) of Sec. II B we obtain for the

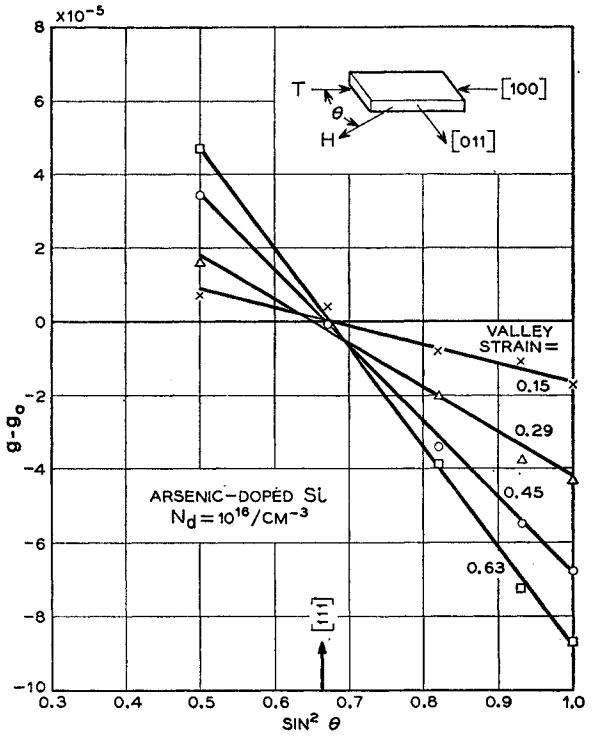

FIG. 9. g shift vs $\sin^2\theta$, where θ is the angle between the stress axis and the magnetic field for a uniaxial compression in the [100] direction for arsenic-doped silicon; $T=1.25$°K, $\nu_e=9$ kMc/sec. The measurements were made in the "parallel squeezor." Since the microwave magnetic field coincides with the stress axis, the electron spin resonance signal decreases rapidly at small values of θ. Hence observations at angles <45° were not possible. Note that the g shift vanishes in the [111] direction. A valley strain of 1.0 is produced by a stress of 9.3 kg/mm² applied in the [100] direction.

TABLE II. Values of g_0 and $g_{\parallel}-g_{\perp}$ for the three donors. The error in the g_0 determination is larger than in the $(g_{\parallel}-g_{\perp})$ determination because of the uncertainty in the field difference between the proton sample and the silicon sample.

Donor	$g_0=\frac{1}{3}g_{\parallel}+\frac{2}{3}g_{\perp}$	$g_{\parallel}-g_{\perp}$
Phosphorus	$1.98850\pm1\times10^{-4}$	$(1.04\pm0.04)\times10^{-3}$
Arsenic	$1.99837\pm1\times10^{-4}$	$(1.10\pm0.05)\times10^{-3}$
Antimony	$1.99858\pm1\times10^{-4}$	$(1.13\pm0.05)\times10^{-3}$

[27] L. Liu and J. C. Phillips (private communication); L. Liu, Phys. Rev. Letters **6**, 683 (1961).

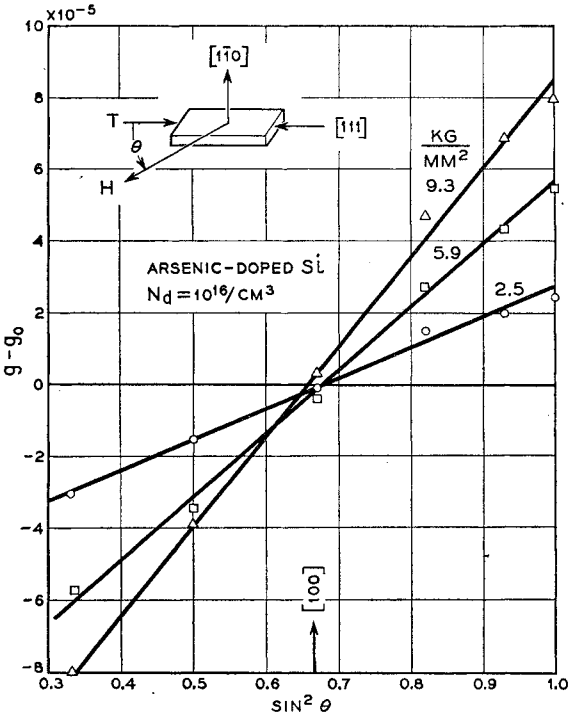

FIG. 10. g shift vs $\sin^2\theta$, where θ is the angle between the magnetic field and the stress axis for a uniaxial compression in the [111] crystallographic direction. The measurements were made on arsenic-doped silicon at 1.25°K, 9 kMc/sec in the "parallel squeezor." This shift is evidence of a change in the one-valley parameters $g_{\parallel}$ and $g_{\perp}$ since no changes in valley populations occur. Notice that the shift vanishes in a [100] crystallographic direction.

matrix element A the value

$$A=0.44\pm0.04. \tag{10}$$

It may seem surprising that the one-valley effect should be roughly as large as the valley repopulation effect. The two main reasons for this are that the Δ_2' band which is admixed by strain lies quite close to the conduction band ($\sim$0.5 ev) and that the value of $g_{\parallel}-g_{\perp}$, which is responsible for the g shift in the valley repopulation effect, is very small in silicon.

Before leaving this section a few remarks about some other consequences of the g anisotropy under strain may be in place. In Part I of this work,[3] we presented experimental data on the substitutional germanium-silicon alloys which at the time were not understood. We had found that a small amount of germanium in silicon ($\sim$1% Ge) produced profound effect on the hf interaction, linewidth, and shape and g value. The explanation seems now obvious: Because of the difference in size between the germanium and silicon atoms, a strain field is produced in the vicinity of the germanium atoms. Donors exposed to these strains will then exhibit the effects discussed in the previous sections, i.e., a g shift and a reduction in the hyperfine splitting. Since the strains are not uniform, a distortion of the line shape is to be expected. It is only because of the small value of $g_{\parallel}-g_{\perp}$ that the resonance is not washed out completely in these alloys. For germanium $g_{\parallel}-g_{\perp}$ is three orders of magnitudes larger[20,21] and there is very little hope of investigating the alloys from the germanium-rich end. This is also exemplified by the observation that dislocations in germanium have a much more pronounced effect,[28] (i.e., line broadening) than in silicon.

Another consequence of the smallness of $g_{\parallel}-g_{\perp}$ is the very long spin-lattice relaxation time observed in silicon at low temperature. This topic is dealt with in the next section.

V. SPIN-LATTICE RELAXATION TIMES

The spin-lattice relaxation time characterizes the rate at which the electronic spin system comes to thermal equilibrium with the lattice. The results of an experimental investigation of several relaxation processes in silicon were presented in a previous publication.[4] At that time the details of the spin-lattice interaction for most of these processes were not understood. In this section we wish to discuss how the static strain experiments are able to shed light on some of the relaxation mechanisms involved. The connection between these two types of experiments is in essence the following: The lattice vibrations represent a time-varying strain which produce an effective interaction. By measuring the change in the paramagnetic resonance spectrum under static strain, one gets a measure of the magnitude of these effective fields which cause the electrons to relax. A detailed analysis of this problem has been carried out by Roth[8] and Hasegawa[9] and will be compared with our experimental results in a subsequent section.

A. The One-Phonon T_s Process

In this section we wish to conisder a relaxation process in which the electron spin flips ($\Delta m_s=\pm1$) without an accompanying nuclear flip ($\Delta m_I=0$). This process is commonly designated by T_s and at low temperatures ($T<2$°K) has been found to be proportional[4,29] to $H^{-4}T^{-1}$. By a one-phonon process we mean that each spin flip is accompanied by the emission or absorption of a single phonon.

1. Experimental Procedure and Results

The experiments were performed on a silicon sample with 10^{15} phosphorus donors/cm^3 at a temperature of 1.25°K. The sample was cut and placed into the cavity in such a manner that the magnetic field could be rotated in the (110) plane. Since T_s at 3000 oe is of the order of hours, we found it more convenient to measure it at 8000 oe. The experimental procedure adopted in all our measurements was as follows. The system was

[28] This may prove to be a convenient tool in studying dislocations.

[29] A. Honig and E. Stupp, Phys. Rev. Letters **1**, 275 (1958).

first saturated (i.e., the electron spin-resonance signal was "erased") at 3000 oe by numerous passages through the resonance lines. The field was then rotated to the appropriate crystallographic direction and raised to 8000 oe at which value the magnetization was left to grow for 5 min. The field was subsequently reduced to 3000 oe, rotated to coincide with the [100] direction, and then swept to observe the amplitude of the resonance signal. Because of the long relaxation times, the time consumed in the intermediate steps did not introduce a significant error in the measurement. At 8000 oe the relaxation time was of the order of 15 min, so that after 5 min the observed magnetization M, given by

$$M=M_0(1-e^{-t/T_s}),$$

depended almost linearly on $1/T_s$. The value of M_0 was accurately determined for the [100], [110], and [111] directions by equilibrating the spin system at 8000 oe for a time which was long compared to 15 min. Special precautions were taken to shield the samples from incident light. This was accomplished by wrapping the cavity with alternate layers of carbon paper and aluminum foil, thus avoiding the introduction of free carriers which could relax the spin systems.

The experimental results are presented in Fig. 11 (see circles) where the relaxation rate $1/T_s$ is plotted against the angle that H makes with the [100] direction. A marked anisotropy is observed which will be compared with the Roth and Hasegawa theories in the next section.

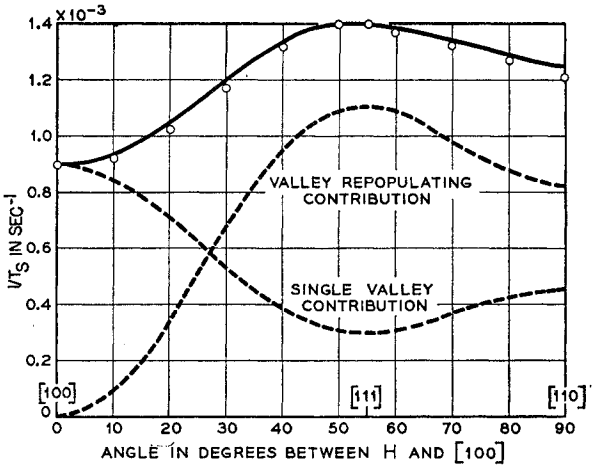

FIG. 11. Relaxation rate $1/T_s$ vs angle between magnetic field and [100] crystallographic direction for phosphorus-doped silicon; $T=1.25$°K, $\nu_e=9$ kMc/sec. The theoretical fit was obtained by normalizing the theoretical expression for the valley repopulation effect [Eq. (11)] and the one-valley effect [Eq. (13)] in such a way that their sum fits the experimental points.

2. Comparison with the Theories of Roth and Hasegawa

An explanation of the T_s relaxation mechanism was given by Roth[8] and Hasegawa.[9] They considered the modulation of the singlet-doublet splitting E_{12} by the lattice vibrations. This represents essentially a time-dependent valley repopulation effect (see Sec. II B) and therefore results in a modulation of the g tensor. The expression for the relaxation rate $1/T_s$ that they obtain for this mechanism with H in the [110] plane is given [see Eqs. (4.17) and (5.4) of reference 9] by

$$\frac{1}{T_s}(\text{valley rep.})=\frac{1}{90\pi}\left(\frac{g_{\parallel}-g_{\perp}}{g_0}\right)^2\left(\frac{\Xi_u}{E_{12}}\right)^2\times\left(\frac{1}{\rho\bar{v}_2{}^5}+\frac{2}{3\rho\bar{v}_1{}^5}\right)\left(\frac{g_0\mu_0H}{\hbar}\right)^4\times(kT)\sin^2\theta(1+3\cos^2\theta),\quad(11)$$

where ρ is the density of Si (2.33 g cm^{-3}), $\bar{v}_2$ is the velocity of the transverse mode (5.42×10^5 cm sec^{-2}), $\bar{v}_1$ is the velocity of the longitudinal mode[15] (9.33×10^5 cm sec^{-2}), and θ is the angle that the magnetic field makes with the [100] direction. Putting in the experimental values for $(g_{\parallel}-g_{\perp})$ and Ξ_u/E_{12} (see Table I and II), one obtains for phosphorus-doped silicon at 1.25°K and 8000 oe with H along the [111] direction

$$1/T_s\ (\text{valley rep.-theory})_{[111]}=0.45\times10^{-3}\ \text{sec}^{-1}.\quad(12)$$

Before making a quantitative comparison of Eqs. (11) and (12) with experiment, we note that this relaxation mechanism alone cannot explain the experimental results since it predicts a zero relaxation rate for H along the [100] direction.

The second relaxation mechanism was explained by Roth.[11] It arises from a modulation of the g shift within one valley, i.e., from the interaction given in Eq. (8). By comparing this interaction with Eq. (30) of reference (8), it can be easily shown [see also Eqs. (4.15) and (5.4) of reference 9] that the resulting relaxation rate is given by

$$\frac{1}{T_s}(\text{one valley})=\frac{1}{20\pi}\left(\frac{A}{g_0}\right)^2\times\left(\frac{1}{\rho\bar{v}_2{}^5}+\frac{2}{3\rho\bar{v}_1{}^5}\right)\left(\frac{g_0\mu_0H}{\hbar}\right)^4\times x(kT)(\cos^4\theta+\tfrac{1}{2}\sin^4\theta),\quad(13)$$

where $A=0.44$ and is the matrix element which we determined previously from the one-valley g shift [see Section IV B2, Eq. (10)]. The rest of the symbols are defined in Eq. (11). Putting in numerical values, we obtain for H along the [111] direction

$$1/T_s\ (\text{one valley-theory})_{[111]}=0.16\times10^{-3}\ \text{sec}^{-1}.\quad(14)$$

We are now finally in a position to compare theory with experiment. In Fig. 11 we have plotted separately the valley repopulation and one-valley contribution to the relaxation rate (see dotted lines) with the angular

dependences given by Eqs. (13) and (15). The normalization of these curves were performed in such a way that the sum of these two rates fits the observed relaxation rate. (see full line). Thus for H along the [111] direction, we obtain the following values for the two relaxation rates:

$$(1/T_s)\ (\text{valley rep.}-\text{exp})_{[111]}=1.1\times10^{-3}\ \text{sec}^{-1}, \quad (15)$$

$$(1/T_s)\ (\text{one valley}-\text{exp})_{[111]}=0.3\times10^{-3}\ \text{sec}^{-1}. \quad (16)$$

A comparison of Eqs. (15) and (16) with Eqs. (12) and (14) shows that the predicted relaxation rates are too slow by about a factor of two. In the field of electron-spin relaxations this would generally be considered a "good" agrement. However, in view of the detailed knowledge of the donor states one may still wonder about the origin of this discrepancy. In this case it may be due to the assumption of an isotropic frequency spectrum of the lattice vibrations and the way the effective transverse acoustical velocity was defined.[9] This would be consistent with the fact that the *ratio* of the valley repopulation to the single-valley rate is in much better agreement with the predicted ratio than the *absolute* value of the individual relaxation rates.

An additional proof of the correctness of the Roth-Hasegawa mechanism is furnished by the experiments on germanium.[21] In this case $(g_{\parallel}-g_{\perp})$ is three orders of magnitude[20] larger and the relaxation rate was found to be correspondingly shorter in agreement with Eq. (11). By straining the sample, the spacing between the ground state and excited state could be altered, thereby enabling us to change the relaxation rate by an order of magnitude.

B. Other Relaxation Processes

1. Comments on the One-Phonon T_x Process

The relaxation process which involves the simultaneous electron nuclear spin flip ($\Delta m_s=\pm1$, $\Delta m_I=\mp1$) is designated by T_x. It has been studied experimentally by several groups[4,30–32] and has been treated theoretically by Pines, Bardeen, and Slichter[33] and Hasegawa.[34]

In principle, one should again be able to derive the relaxation rate from the observed change in the hf interaction with applied stress. In Sec. IV A we have found that the observed change in $|\Psi(0)|^2$ is quadratic in the deformation under the application of uniaxial stress [see Eq. (2)]. It can be shown[34] that such a quadratic dependence cannot lead to a one-phonon relaxation process. However, under the application of an applied uniaxial "biasing" stress (or built-in stress due to imperfections), the change in $|\Psi(0)|^2$ would be first order in strain and hence capable of producing a one-phonon T_x process. The effectiveness of this T_x mechanism will thus depend on the magnitude of the applied strain.

In order to prove the correctness of the above ideas, T_x was measured in an arsenic-doped sample ($\sim10^{16}$ As/cm^3) subjected to varying amounts of strain. At zero applied strain, T_x at 1.2°K and 3000 oe was found to be $\sim3\times10^3$ sec. By applying a uniaxial stress (in the [100] direction) corresponding to a valley strain of $x=0.8$, the magnitude of T_x dropped to $\sim10^2$ sec.

As a consequence of the strain dependence of T_x, care has to be taken to avoid built-in strains when investigating these processes. The disagreement in the literature between the various values[4,30–32] of T_x may be the result of varying amounts of built-in strains. The ability to increase the effectiveness of T_x by applying a uniaxial strain should prove important in nuclear orientation schemes in which T_x plays a dominant role.[30,33]

In order to understand the T_x process at zero strain, Pines, Bardeen, and Slichter[33] calculated a one-phonon process by assuming a linear change in $|\Psi(0)|^2$ under *uniform* dilation given by the expression

$$|\Delta\Psi(0)|^2/|\Psi(0)|^2=\gamma s, \quad (17)$$

where s is the strain and γ was estimated by PBS to have a value of ~50. Their theory proved to be in fair agreement with the experimental values.[4,30–32] More recently Paul[35] has measured the change in the ionization energy and dielectric constant with hydrostatic pressure and found $dE_i/dP=-10^{-14}$ ev dyne^{-1} cm^2 and $dK/dP=-7\times10^{-13}$ dyne^{-1} cm^2. From these values it can be shown that the above estimate of γ is about two orders of magnitude too large. It seems therefore that the agreement of the experimentally measured values[4,30–32] of T_x with the theoretical estimate of PBS is fortuitious. An additional experimental check of the value of γ was obtained by applying a uniaxial stress in the [111] direction (thereby eliminating the valley repopulation effect) and looking for the change in the hyperfine splitting. From these experiments we conclude that $\gamma<2$ which is consistent with the measurements of Paul.[35]

The donor electron interacts also with the Si^{29} nuclei. The hfs with these nuclei is *linear* in strain.[5] We have measured the hfs of the Si^{29} nuclei in the (440) lattice positions[3,36] in a sample subjected to a uniaxial stress in the [100] direction. The value of γ obtained for this site was 60 ± 5. It can be shown[33] that because of the smallness of the hyperfine interaction, its modulation by lattice vibrations also does not result in a significant relaxation rate.

[30] A. Abragam and J. Combrisson, Compt. rend. **243**, 576 (1956).
[31] J. W. Culvahouse and F. M. Pipkin, Phys. Rev. **109**, 319 (1958).
[32] A. Honig and E. Stupp, Phys. Rev. **117**, 69 (1960).
[33] D. Pines, Bardeen, and Slichter, Phys. Rev. **106**, 489 (1957).
[34] H. Hasegawa (to be published).
[35] W. Paul, J. Phys. Chem. Solids **8**, 196 (1959).
[36] In reference 3 we presented a detailed analysis of the hf interaction with the different Si^{29} nuclei and pointed out the difficulties encountered in assigning the correct lattice positions to the nuclei. The application of a uniaxial stress would have made the identification procedure much easier.

It seems, therefore, that at zero external strain, one-phonon processes are not effective in determining T_x at the temperatures and fields under consideration.

2. *Raman-Type Processes*

By a Raman-type process we mean a two-step process in which a phonon of frequency ω' is absorbed and a phonon of frequency ω'' is emitted, such that $h(\omega'-\omega'')=h\omega$, where ω is the Larmor frequency of the electron spin.

In the preceding section we pointed out that the quadratic dependence of $|\Delta\Psi(0)|^2$ precludes a single-phonon T_x process. However, Raman processes are allowed and, as shown by Honig and Stupp,[32] predominate above 2.2°K. Below this temperature their results are inconclusive. Hasegawa[34] has calculated the Raman-type T_x process and obtains a good agreement with the experimental results down to 1.2°K.

From the temperature dependence of the T_s process above 2.5°K (i.e., $T_s \simeq T^{-7}$) one also concludes that Raman processes must be responsible for the observed relaxation rate in this temperature region. Roth[8] has calculated this process and predicts, besides the T^{-7} dependence, an anisotropy in T_s similar to that for the one-phonon process (see Sec. V) and a quadratic field dependence. We have checked the field and angular dependence of T_s in this temperature range and found it to be isotropic and independent of H between 3000 and 8000 oe. This discrepancy between the theory and experiment is not understood at present.

ACKNOWLEDGMENTS

We would like to thank L. Roth, H. Hasegawa, W. Kohn, M. Lax, Y. Yafet, and E. Abrahams for many helpful comments and discussions and E. A. Gere for his assistance in the measurements. In particular, it is a pleasure to acknowledge the stimulation received from L. Roth and H. Hasegawa whose theories prompted us to look for the anisotropy in T_s. One of the authors, (D.K.W.), would like to express particular appreciation to the Transistor Device Development Group at the Bell Telephone Laboratories for their generous encouragement of this work.

APPENDIX

A. Donor Electron Wave Functions in Silicon and the Valley-Orbit Matrix

The general form of the wave function $\Psi(\mathbf{r})$ for the bound donor electrons is of the form,[2,5]

$$\Psi(\mathbf{r})=\sum_{j=1}^{6}\alpha^{(j)}F^{(j)}(\mathbf{r})u^{(j)}(\mathbf{r})\exp(i\mathbf{k}_0{}^{(j)}\cdot\mathbf{r}), \quad \text{(A1)}$$

where $u^{(j)}(\mathbf{r})\exp(i\mathbf{k}_0{}^{(j)}\cdot\mathbf{r})$ is the conduction-band Bloch function at the jth valley, $F^{(j)}(\mathbf{r})$ is the hydrogen-like modulating function, and $|\alpha^{(j)}|^2$ determines the probability of finding the electron in the jth valley. Because there are six valleys, there are correspondingly six different valley arrangements for any given solution of the modulation envelope $F(\mathbf{r})$ including the $1s$-like ground state. From group theory one finds that the six states can be split in a cubic crystal into a singlet, doublet, and triplet.

The valley compositions for the various levels can be written in the following tensor form[5]:

$$\begin{aligned}
&\text{Singlet} && (\alpha_{11}{}^{(j)})=(1/\sqrt{6})(1,\,1,\,1,\,1,\,1,\,1),\\
&\text{Doublet} && (\alpha_{21}{}^{(j)})=(1/\sqrt{12})(2,\,2,\,-1,\,-1,\,-1,\,-1),\\
&&& (\alpha_{22}{}^{(j)})=(1/\sqrt{4})(0,\,0,\,1,\,1,\,-1,\,-1),\\
&\text{Triplet} && (\alpha_{31}{}^{(j)})=(1/\sqrt{2})(1,\,-1,\,0,\,0,\,0,\,0),\\
&&& (\alpha_{32}{}^{(j)})=(1/\sqrt{2})(0,\,0,\,1,\,-1,\,0,\,0),\\
&&& (\alpha_{33}{}^{(j)})=(1/\sqrt{2})(0,\,0,\,0,\,0,\,1,\,-1).
\end{aligned} \quad \text{(A2)}$$

The electronic wave function of the singlet state distinguishes itself from the one associated with the doublet and triplet states by having a finite value at the donor nucleus. This results in depressing the singlet state with respect to the others. The interaction term responsible for this depression is called the valley-orbit term and appears in the donor electron Hamiltonian in in a matrix form similar to that for the spin-orbit for a single electron. If we concern ourselves only with the splitting of the various levels from the center of gravity, then the unstrained valley-orbit (vo) matrix is[6]

$$-H_{\mathrm{vo}}=\begin{vmatrix}
0 & (1+\delta)\Delta_c & \Delta_c & \Delta_c & \Delta_c & \Delta_c\\
(1+\delta)\Delta_c & 0 & \Delta_c & \Delta_c & \Delta_c & \Delta_c\\
\Delta_c & \Delta_c & 0 & (1+\delta)\Delta_c & \Delta_c & \Delta_c\\
\Delta_c & \Delta_c & (1+\delta)\Delta_c & 0 & \Delta_c & \Delta_c\\
\Delta_c & \Delta_c & \Delta_c & \Delta_c & 0 & (1+\delta)\Delta_c\\
\Delta_c & \Delta_c & \Delta_c & \Delta_c & (1+\delta)\Delta_c & 0
\end{vmatrix}. \quad \text{(A3)}$$

If we operate with this matrix on the various valley tensors (A2) we find the doublet lies $E_{12}=6\Delta_c$ above the singlet. We have also introduced the term δ to provide for the fact that the doublet and triplet may be displaced by an energy difference E_{23}. In any case, this displacement should be very small and amounts to $E_{23}=2\delta\Delta_c$ for the above form of the valley-orbit matrix.

B. Valley Shifts for Uniaxial Compression

The form for the strain components resulting from a uniaxial compressive stress T applied in a [100] direction in a cubic crystal is

$$u_{\alpha\beta}=\begin{vmatrix} S_{11} & S_{12} & S_{12} & 0 & 0 & 0 \\ S_{12} & S_{11} & S_{12} & 0 & 0 & 0 \\ S_{12} & S_{12} & S_{11} & 0 & 0 & 0 \\ 0 & 0 & 0 & \tfrac{1}{2}S_{44} & 0 & 0 \\ 0 & 0 & 0 & 0 & \tfrac{1}{2}S_{44} & 0 \\ 0 & 0 & 0 & 0 & 0 & \tfrac{1}{2}S_{44} \end{vmatrix} \begin{vmatrix} T \\ 0 \\ 0 \\ 0 \\ 0 \\ 0 \end{vmatrix}, \quad \text{(B1)}$$

where the S_{ij}'s are the appropriate stiffness coefficients. If we apply Herring's[23,24] deformation potential analysis, the energy shift of the jth valley is given by

$$E^{(j)}=[\Xi_d\delta_{\alpha\beta}+\Xi_u k_\alpha{}^{(j)}k_\beta{}^{(j)}]u_{\alpha\beta}, \quad \text{(B2)}$$

where the $k_\alpha{}^{(j)}$ are the components of a unit vector pointing from the center of the Brillouin zone to the jth valley, and the deformation potentials Ξ_d and Ξ_u are defined as follows: Ξ_d is the valley shift due to a dilation in the two directions normal to the valley axis, and Ξ_u is the shift due to a uniaxial shear compounded of a stretch along the valley axis and a contraction in the two normal directions.

Solving for the shift in energy of the two valleys in the direction of the applied stress, we have

$$E^1=E^2=[\Xi_d(S_{11}+2S_{12})+\Xi_u S_{11}]T. \quad \text{(B3)}$$

The four valleys normal to the stress are shifted

$$E^3=E^4=E^5=E^6=[\Xi_d(S_{11}+2S_{12})+\Xi_u S_{12}]T. \quad \text{(B4)}$$

We can readily solve for the shift in energy of the center of gravity of the six valleys:

$$E_{\text{c.g.}}=[3\Xi_d(S_{11}+2S_{12})+\Xi_u(S_{11}+2S_{12})]T/3. \quad \text{(B5)}$$

Subtracting this from the previous results, one obtains the energy displacement of the conduction band valleys from the band edge produced by a [100] uniaxial compression:

$$E^{1,2}-E_{\text{c.g.}}=(1/3)\Xi_u s', \quad \text{(B6)}$$

$$E^{3,4,5,6}-E_{\text{c.g.}}=-(1/6)\Xi_u s', \quad \text{(B7)}$$

where $s'=2(S_{11}-S_{12})T$.

C. Donor Wave Functions and Valley-Orbit Matrix Under Strain

The energy-shift terms for the various conduction-band valleys will appear as diagonal elements of the valley-orbit matrix (A3). We will henceforth assume that the only effect of the applied strain is to shift the valley populations. Then the matrix for the case of a [100] uniaxial compression becomes

$$-H_{\text{vo}}=\begin{vmatrix} (-1/3)\Xi_u s' & (1+\delta)\Delta_c & \Delta_c & \Delta_c & \Delta_c & \Delta_c \\ (1+\delta)\Delta_c & (-1/3)\Xi_u s' & \Delta_c & \Delta_c & \Delta_c & \Delta_c \\ \Delta_c & \Delta_c & (1/6)\Xi_u s' & (1+\delta)\Delta_c & \Delta_c & \Delta_c \\ \Delta_c & \Delta_c & (1+\delta)\Delta_c & (1/6)\Xi_u s' & \Delta_c & \Delta_c \\ \Delta_c & \Delta_c & \Delta_c & \Delta_c & (1/6)\Xi_u s' & (1+\delta)\Delta_c \\ \Delta_c & \Delta_c & \Delta_c & \Delta_c & (1+\delta)\Delta_c & (1/6)\Xi_u s' \end{vmatrix} \quad \text{(C1)}$$

$$=\Delta_c\begin{vmatrix} -2x & 1+\delta & 1 & 1 & 1 & 1 \\ 1+\delta & -2x & 1 & 1 & 1 & 1 \\ 1 & 1 & x & 1+\delta & 1 & 1 \\ 1 & 1 & 1+\delta & x & 1 & 1 \\ 1 & 1 & 1 & 1 & x & 1+\delta \\ 1 & 1 & 1 & 1 & 1+\delta & 1 \end{vmatrix}, \quad \text{(C2)}$$

where $x=\Xi_u s'/6\Delta_c$ is the quantity we have called the "valley strain." It is apparent from the form of H_{vo} that the only wave functions intermixed by this strain are those characterized by the valley populations $\alpha_{11}{}^{(j)}$ and $\alpha_{21}{}^{(j)}$ [see Eq. (A2)]. This means that the only two levels mixed by strain are the singlet and one component of the doublet. The two new valley composition arising from this mixture may be characterized by $\alpha_{\text{strain}}{}^{(j)}$ which must have the form

$$\alpha_{\text{strain}}{}^{(j)}=(\alpha_A,\alpha_A,\alpha_B,\alpha_B,\alpha_B,\alpha_B), \quad \text{(C3)}$$

where α_A and α_B are numerical coefficients to be determined. For the rest of the levels the valley populations remain unaltered and are given by equation (A2). If we substitute $\alpha_{\text{strain}}{}^{(j)}$ into the Schrödinger equation $H_{\text{vo}}\Psi(r)=E_{\text{vo}}\Psi(r)$, we get

$$4(\alpha_B)^2-2(\alpha_A)^2=(3x+2)\alpha_A\alpha_B. \tag{C4}$$

The normalization of the valleys requires that

$$4(\alpha_B)^2+2(\alpha_A)^2=1. \tag{C5}$$

Solving for the valley populations under a [100] uniaxial compression, we obtain

$$\begin{aligned}(\alpha_A)^2&=\tfrac{1}{4}[1\mp(x+\tfrac{2}{3})(x^2+\tfrac{4}{3}x+4)^{-\frac{1}{2}}],\\ (\alpha_B)^2&=\tfrac{1}{8}[1\pm(x+\tfrac{2}{3})(x^2+\tfrac{4}{3}x+4)^{-\frac{1}{2}}].\end{aligned} \tag{C6}$$

The upper sign describes the ground state (designated as $\epsilon^{-}{}_{11,21}$ in Fig. 1), the lower sign the higher lying state. From Eq. (C6) it is seen that for large compressive stresses ($-x\gg1$) an electron in its ground state spends all its time in the two depressed valleys.

Knowing the valley compositions for all the levels under strain, it is possible to solve for the energy of the various levels. For the two admixed states we find

$$\begin{aligned}\epsilon^{-}{}_{11,21}&=\Delta_c[-(2+\delta)+\tfrac{1}{2}x-\tfrac{3}{2}(x^2+\tfrac{4}{3}x+4)^{\frac{1}{2}}],\\ \epsilon^{+}{}_{11,21}&=\Delta_c[-(2+\delta)+\tfrac{1}{2}x+\tfrac{3}{2}(x^2+\tfrac{4}{3}x+4)^{\frac{1}{2}}],\end{aligned} \tag{C7}$$

where the upper equation refers to the ground state. The relation between Δ_c and δ to the singlet-doublet and doublet-triplet splitting is indicated in Fig. 1. The energies of the other excited states depend on the valley strain as follows:

$$\begin{aligned}\epsilon_{22}&=\Delta_c[(1-\delta)-x],\\ \epsilon_{31}&=\Delta_c[(1+\delta)+2x],\\ \epsilon_{32}=\epsilon_{33}&=\Delta_c[(1+\delta)-x].\end{aligned} \tag{C8}$$

These results are plotted in Fig. 1 for the case where δ is assumed to be small and positive.

D. Hyperfine Splitting under Strain

There are two terms appearing in the spin Hamiltonian for the donor electrons whose change under strain we will consider. The first of these is the Fermi-Segrè interaction given by

$$(8/3)\pi\mathfrak{y}_e\cdot\mathfrak{y}_n|\Psi(0)|^2, \tag{D1}$$

which is the dominant contribution to the hyperfine splitting for the 1s-like states under consideration. $\mathfrak{y}_e$ is the electron magnetic moment, $\mathfrak{y}_n$ is the magnetic moment of the impurity nucleus, and $|\Psi(0)|^2$ is the square of the electronic wave function at the donor nucleus.

Using the effective-mass expression for the wave function [see Eq. (A1)], we get for the hyperfine splitting (hfs)

$$\text{hfs}=(8\pi/3)\mathfrak{y}_e\cdot\mathfrak{y}_n|F^{(j)}(0)|^2|u^{(j)}(0)|^2|\textstyle\sum\alpha^{(j)}|^2. \tag{D2}$$

Assuming that the only effect of the strain is to alter the valley populations, we obtain for the ratio of the hyperfine splitting of a sample under strain $(\text{hfs})_s$ to the hyperfine splitting in an unstrained sample $(\text{hfs})_0$,

$$(\text{hfs})_s/(\text{hfs})_0=\tfrac{1}{6}|\textstyle\sum\alpha^{(j)}|^2. \tag{D3}$$

For an uniaxial compression in the [100] direction, we can substitute the value for α_{strain} from (C3) for the ground state and find that

$$(\text{hfs})_s/(\text{hfs})_0=\tfrac{1}{2}[1+(2+\tfrac{1}{3}x)(x^2+\tfrac{4}{3}x+4)^{-\frac{1}{2}}]. \tag{D4}$$

The above expression shows that the hfs in the limiting cases is proportional to the number of occupied valleys, i.e., the ratio of splitting approaches 2/3 for large tensile stresses ($x\gg1$) and 1/3 for large compressive stresses ($-x\gg1$). For small stresses the result reduces to a quadratic expression

$$(\text{hfs})_s/(\text{hfs})_0=1-x^2/18+\cdots, \tag{D5}$$

as previously discussed by Kohn.[5] From this we see that "valley strains" of the order of unity should result in changes in the hfs greater than 5%, a readily detectable change.

E. Electronic g Value in the Absence of Strain

The term in the spin Hamiltonian which leads to the microwave transition energy (i.e., center of gravity of the hyperfine spectrum) is of the form

$$\mathbf{S}\cdot\mathbf{g}\cdot\mathbf{H}, \tag{E1}$$

where $\mathbf{S}$ is the spin of the electron, $\mathbf{H}$ is the applied magnetic field, and $\mathbf{g}$ is the tensor form of the electronic g. For an electron in a single jth valley we can write it as

$$\mathbf{g}^{(j)}=\begin{vmatrix} g_\perp & & \\ & g_\perp & \\ & & g_{11}\end{vmatrix}, \tag{E2}$$

where the principal axes of this tensor coincide with the axes of the effective-mass tensor. Expression (E2) leads to an anisotropic g value given by

$$g^2=g_{11}{}^2\cos^2\theta+g_\perp{}^2\sin^2\theta, \tag{E3}$$

where θ is the angle between the magnetic field and the major valley axis. Because of the multivalley nature of silicon we will show that the measured g value is isotropic. Following Hasegawa,[9] we rewrite (E2) as

$$\begin{aligned}\mathbf{g}^{(j)}&=g_\perp\begin{vmatrix}1&&\\&1&\\&&1\end{vmatrix}+(g_{11}-g_\perp)\begin{vmatrix}0&&\\&0&\\&&1\end{vmatrix}\\ &=g_\perp\mathbf{I}+(g_{11}-g_\perp)\mathbf{U}^{(j)}.\end{aligned} \tag{E4}$$

The measured electronic g value is obtained from the single-valley g tensor by averaging $\mathbf{S}\cdot\mathbf{g}\cdot\mathbf{H}$ over all the valleys in accordance with the respective valley populations as given by (A2).

$$\mathbf{g}\cdot\mathbf{S}\cdot\mathbf{H}=\langle\mathbf{S}\cdot\mathbf{g}^{(j)}\cdot\mathbf{H}\rangle_{\mathrm{av}}$$
$$=\mathbf{S}\cdot\{\textstyle\sum_j(\alpha^{(j)})^2[(g_\perp\mathbf{I}+(g_\parallel-g_\perp)\mathbf{U}^{(j)}]\}\cdot\mathbf{H}. \quad \text{(E5)}$$

For the unstrained ground state, all valleys have equal populations and Eq. (E5) becomes

$$g_0\mathbf{S}\cdot\mathbf{H}=\mathbf{S}\cdot[g_\perp+(2/6)(g_\parallel-g_\perp]\mathbf{I}\cdot\mathbf{H}$$
$$=(\tfrac{1}{3}g_\parallel+\tfrac{2}{3}g_\perp)\mathbf{S}\cdot\mathbf{H}; \quad \text{(E6)}$$

i.e., the measured g is isotropic and is given by

$$g_0=\tfrac{1}{3}g_\parallel+\tfrac{2}{3}g_\perp. \quad \text{(E7)}$$

F. Electronic g Value in the Presence of Strain

In order to obtain the electronic g value under the application of a compressive stress along the [100] direction, we substitute the valley population given by (C6) into (E5)

$$g(\mathbf{S}\cdot\mathbf{H})=\mathbf{S}\cdot\begin{vmatrix} g_\perp+2(g_\parallel-g_\perp)(\alpha_B)^2 & & \\ & g_\perp+2(g_\parallel-g_\perp)(\alpha_B)^2 & \\ & & g_\perp+2(g_\parallel-g_\perp)(\alpha_A)^2 \end{vmatrix}\cdot\mathbf{H} \quad \text{(F1)}$$

$$=\mathbf{S}\cdot\begin{vmatrix} g_\perp' & & \\ & g_\perp' & \\ & & g_\parallel' \end{vmatrix}\cdot\mathbf{H}. \quad \text{(F2)}$$

Comparing the above expression with the single-valley result [(E2), (E3)], we obtain for the measured g value under strain

$$g^2=(g_\parallel')^2\cos^2\theta+(g_\perp')^2\sin^2\theta, \quad \text{(F3)}$$

where $g_\parallel'$ and $g_\perp'$ are the "effective" g values whose magnitude will depend on the valley strain and the "real" $g_\parallel$ and $g_\perp$. Substituting the values for α_A and α_B [Eq. (C6)] into (F1) and recalling that $\sum_j(\alpha^{(j)})^2=1$, we obtain

$$g^2=g_\perp^2\left\{1+\left(\frac{g_\parallel-g_\perp}{g_\perp}\right)[4(\alpha_A)^2(1-\tfrac{3}{2}\sin^2\theta)+\sin^2\theta]\right.$$
$$\left.+\text{terms in }\left(\frac{g_\parallel-g_\perp}{g_\perp}\right)^2\right\}. \quad \text{(F4)}$$

Retaining only the first-order terms [since $(g_\parallel-g_\perp)/g\simeq10^{-3}$ for donors in silicon] and using the relation $g_0=\frac{1}{3}g_\parallel+\frac{2}{3}g_\perp$, we obtain for the shift of the g value from its unstrained value

$$g-g_0=(g_\parallel-g_\perp)(1-\tfrac{3}{2}\sin^2\theta)[2(\alpha_A)^2-\tfrac{1}{3}]. \quad \text{(F5)}$$

Substituting the value for $(\alpha_A)^2$ for the ground state under a [100] uniaxial compression [Eq. (C6)], we arrive at the final result

$$g-g_0=\tfrac{1}{6}(g_\parallel-g_\perp)(1-\tfrac{3}{2}\sin^2\theta)$$
$$\times[1-(3x+2)(x^2+\tfrac{4}{3}x+4)^{-\frac{1}{2}}]. \quad \text{(F6)}$$

For large compressive stresses ($-x\gg1$), Eq. (F6) becomes

$$g-g_0=\tfrac{2}{3}(g_\parallel-g_\perp)(1-\tfrac{3}{2}\sin^2\theta). \quad \text{(F7)}$$

In this case, for H parallel to the applied stress (i.e., along the major valley axis) we have

$$g=g_0+\tfrac{2}{3}(g_\parallel-g_\perp)=g_\parallel; \quad \text{(F8)}$$

and for H perpendicular to the stress,

$$g=g_0-\tfrac{1}{3}(g_\parallel-g_\perp)=g_\perp. \quad \text{(F9)}$$

This is to be expected since, for large compressive stresses in the [100] direction, one approaches the situation in which the electron spends its time in two opposite valleys.

G. Breit-Rabi Corrections

The magnetic interaction of an electron with spin $S=\frac{1}{2}$ and its nucleus with spin I is given by the Hamiltonian

$$=a\mathbf{I}\cdot\mathbf{S}+g\mu_0\mathbf{S}\cdot\mathbf{H}-g_I\mu_0\mathbf{I}\cdot\mathbf{H}, \quad \text{(G1)}$$

where a is the hyperfine interaction constant and H the applied magnetic field. Since we are only interested in *changes* in g and a under strain, we can neglect the last (nuclear) term. The eigenvalues $W(F,m_F)$ are given by the Breit-Rabi[37] equation

$$W(F,m_F)=-\tfrac{1}{2}\Delta E/(2I+1)\pm\tfrac{1}{2}\Delta E$$
$$\times[1+\Delta m_F x/(2I+1)+x^2]^{\frac{1}{2}}, \quad \text{(G2)}$$

where $F=I\pm\frac{1}{2}$. The positive sign corresponds to $I+\frac{1}{2}$ and the negative to $I-\frac{1}{2}$; $m_F=m_I\pm\frac{1}{2}$. The zero-field splitting is $\Delta E=a(I+\frac{1}{2})$ and $x=g\mu_0H/\Delta E$. The microwave field of frequency ν will induce transitions between levels $\Delta F=\pm1$, $\Delta m_F=\pm1$ (i.e., $\Delta m_s=\pm1$; $\Delta m_I=0$). From Eq. (G2) we find the energy of these transitions to order $(a/g\mu H)^2$:

$$h\nu=E_{m_F}-E_{m_{F-1}}=g\mu_0H$$
$$\times\{1+\tfrac{1}{2}(a/g\mu H)^2[I(I+1)-m_I^2]\}+m_Ia, \quad \text{(G3)}$$

or for the measured magnetic field H

$$H=(g\mu_0/h\nu)\{1-\tfrac{1}{2}(a/g\mu_0H)^2[I(I+1)-m_I^2]\}-m_Ia. \quad \text{(G4)}$$

Experimentally we measure the two resonance fields corresponding to the $m_I=\pm\frac{1}{2}$ transitions. From (G4) we find that the hyperfine interaction in terms of these

[37] G. Breit and I. I. Rabi, Phys. Rev. 38, 2082 (1931).

fields is given by

$$a=-g\mu_0(H_{m_{I=\frac{1}{2}}}-H_{m_{I=-\frac{1}{2}}}), \quad \text{(G5)}$$

i.e., no corrections are necessary.

From the average of the two fields $H_{m_{I=\frac{1}{2}}}$ and $H_{m_{I=-\frac{1}{2}}}$ we can define a measured g value, g_m, given by

$$h\nu=\tfrac{1}{2}\mu_0 g_m(H_{m_{I=+\frac{1}{2}}}+H_{m_{I=-\frac{1}{2}}}). \quad \text{(G6)}$$

Comparing this expression with (G3), we obtain for the true g value

$$g=g_m\{1-\tfrac{1}{2}(a/g\mu H)^2[I(I+1)-\tfrac{1}{4}]\}. \quad \text{(G7)}$$

If we subject the sample to a compressive stress changing the hyperfine splitting a, then the differential correction to g is given by

$$\Delta g=2(g_m-g)(\Delta a/a). \quad \text{(G8)}$$

PHYSICAL REVIEW VOLUME 124, NUMBER 4 NOVEMBER 15, 1961

Electron Spin Resonance Studies in SiC

H. H. WOODBURY AND G. W. LUDWIG
General Electric Research Laboratory, Schenectady, New York

(Received July 13, 1961)

Electron spin resonance studies have been made on boron and nitrogen as impurities in 6*H* silicon carbide. It is concluded that both impurities substitute for carbon and that they occupy the three nonequivalent carbon sites with equal probability. Hyperfine structure is well resolved for both species. The pattern for boron occupying one site is unusual in that the hyperfine splitting vanishes when the applied field is about 50° from the hexagonal axis of the crystal. The nitrogen hyperfine structure is interpretable in terms of some *s* character for the unpaired electron, while the boron hyperfine structure indicates predominantly *p* character.

I. INTRODUCTION

THE basic arrangement of atoms in Column IV semiconductors such as Ge, Si, and SiC is tetrahedral. An atom of a Column V element normally acts as a donor in such semiconductors since it has one valence electron left over after completing the normal tetrahedral bonding. At sufficiently low temperatures this electron is localized near the donor atom; at high temperatures it can ionize and give rise to *n*-type conduction. Similarly, an atom of a Column III element acts as an acceptor and gives rise to *p*-type conduction.

Most semiconductors, including silicon carbide, are intrinsically diamagnetic; the perfect crystal has no unpaired electrons and does not show spin resonance absorption. However, many impurities introduced into such semiconductors are paramagnetic and result in spin resonance absorption. The Column III and Column V elements act as such impurities in the Column IV semiconductors. The Column V elements, P, As, Sb, and Bi, have been extensively studied by spin resonance in Si.[1] Resonance of the first three donors has recently been reported in Ge[2,3]; the Column V element nitrogen has been studied in diamond.[4] Column III elements have recently been observed in Si subjected to uniaxial stress.[5]

Spin resonance of Column V and Column III elements in SiC has been reported by van Wieringen.[6] He attributed a three-line spectrum in *n*-type material to nitrogen and a single-line spectrum in *p*-type material to Column III acceptors. This was the first report of resonances due to N and Column III acceptors in a Column IV semiconductor. In this paper we report on further studies of N- and B-doped SiC. A preliminary account of our experiments has already been given.[7]

The spin resonance spectrometer used to study SiC operates at a microwave frequency ν of about 14 kMc/sec. Thus the magnetic field H for resonance is of order 5000 gauss for systems (including N and B in SiC) with g factors near that of the free electron. Some measurements were made at 20 kMc/sec with a correspondingly higher field. The electron-nuclear double resonance technique[1] has also been employed. Details of the experimental equipment have been given elsewhere.[8]

The SiC crystals studied were small hexagonal single

[1] G. Feher, Phys. Rev. **114**, 1219 (1959).
[2] G. Feher, D. K. Wilson, and E. A. Gere, Phys. Rev. Letters **3**, 25 (1959).
[3] R. E. Pontinen and T. M. Sanders, Jr., Phys. Rev. Letters **5**, 311 (1960).
[4] W. V. Smith, P. P. Sorokin, I. L. Gelles, and G. J. Lasher, Phys. Rev. **115**, 1546 (1959).
[5] G. Feher, J. C. Hensel, and E. A. Gere, Phys. Rev. Letters **5**, 309 (1960).
[6] J. S. van Wieringen, in *Semiconductors and Phosphors*, edited by M. Schön and H. Welker (Interscience Publishers, Inc., New York, 1958), p. 367.
[7] H. H. Woodbury and G. W. Ludwig, Bull. Am. Phys. Soc. **4**, 144 (1959).
[8] G. W. Ludwig and H. H. Woodbury, Phys. Rev. **113**, 1014 (1959); H. H. Woodbury and G. W. Ludwig, *ibid.* **117**, 102 (1960).

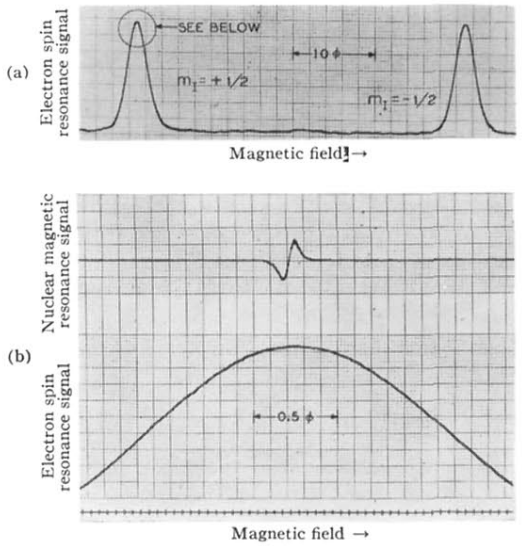

FIG. 4. Illustration of the method used for the accurate determination of the hfs and the electronic g value. (a) Hyperfine spectrum of phosphorus donors in silicon; $N_d = 10^{16}/\text{cm}^3$, $T = 1.25°\text{K}$ $\nu_e \simeq 9$ kMc/sec. (b) Portion of the $m_I = +\frac{1}{2}$ line which is shown encircled in (a). The field marker shown is derived from a proton sample. The centers of the lines were determined with an accuracy of ~ 10 millioersteds.